Washington, D.C.:American Statistical Association, pp. 12–18, 1985.
[10] D. Geiger and A. Yuille, "A common framework for image segmentation by energy functions and nonlinear diffusion," MIT AI Lab, 1989
[11] S. Grossberg, "Neural dynamics of brightness perception: Features, boundaries, diffusion, and resonance." Perception and Psychophysics, vol. 36, no. 5, pp. 428–456, 1984.
[12] Y.-S. Han and W.E. Snyder, "Adaptive edge-preserving smoothing via adaptive mean field annealing," Proc. SPIE '92, Conf. on Neural and Stochastic Neural Methods in Image and Signal Processing, San Diego, Calif., 1992.
[13] T. Hebert and R. Leahy, "A generalized EM algorithm for 3D Bayesian reconstruction from Poisson data using Gibbs priors," IEEE Trans. Medical Imaging, June 1989.
[14] H. Hiriyannaiah, G. Bilbro, W. Snyder, and R. Mann, "Restoration of locally homogeneous images using mean field annealing," J. Optical Soc. of America A, pp. 1,901–1,912, Dec. 1989.
[15] R. Kashyap and R. Chellappa, "Estimation and choice of neighbors in spatial-interaction model of images," IEEE Trans. Information Theory, vol. 29, pp. 60–72, Jan. 1983.
[16] S. Kirkpatrick, C. Gelatt, and M. Vecchi, "Optimization by simulated annealing," Science, vol. 220, pp. 671–668, 1983.
[17] A. Kolmogorov, A. "On the representation of continuous functions of one variable by superposition of continuous functions of one variable and addition" AMS Translation, vol. 2, pp. 55–59, 1957.
[18] P. Morris, Nuclear Magnetic Resonance Imaging in Medicine and Biology. Oxford, England: Clarendon Press, 1986.
[19] N. Nordström, "Biased anisotropic diffusion—a unified regularization and diffusion approach to edge detection," Image and Vision Computing, vol. 8, no. 4, pp. 318–327, 1990.
[20] P. Perona and J. Malik, "Scale-space and edge detection using anisotropic diffusion," IEEE Trans. Pattern Analysis and Machine Intelligence, vol. 12, pp. 429–439, 1990.
[21] R. Bart ter Haar, ed., Geometry-Driven Diffusion in Computer Vision (Computational Imaging and Vision Series). Dordrecht, Netherlands: Kluwer, 1994.
[22] R. Whitaker, "Geometry-limited diffusion in the characterization of geometric patches in images," TR91-039, Dept. of Computer Science, Univ. of North Carolina, Chapel Hill, 1991.
[23] G. Wolberg and T. Pavlidis, "Restoration of binary images using stochastic relaxation with annealing," Pattern Recognition Letters, vol. 3, no. 6, pp. 375–388, Dec. 1985.

Discontinuity-Preserving and Viewpoint Invariant Reconstruction of Visible Surfaces Using a First Order Regularization

June H. Yi and David M. Chelberg

***Abstract*—This paper describes the application of a first order regularization technique to the problem of reconstruction of visible surfaces. Our approach is a computationally efficient first order method that simultaneously achieves approximate invariance and preservation of discontinuities. Our reconstruction method is also robust with respect to the smoothing parameter λ. The robustness property to λ allows a free choice of the smoothing parameter λ without struggling to determine an optimal λ that provides the best reconstruction. A new approximately invariant first order stabilizing function for surface reconstruction is obtained by employing a first order Taylor expansion of a nonconvex invariant stabilizing function that is expanded at the estimated value of the squared gradient instead of at zero. The data compatibility measure used is the squared perpendicular distance between the reconstructed surface and the constraint surface. This combination of stabilizing function and data compatibility measure is necessary to achieve invariance with respect to rotations and translations of the surfaces being reconstructed. Sharp preservation of discontinuities is achieved by a weighted sum of adjacent pixels such that the adjacent pixels that are more likely to be in different regions are less weighted. The results indicate that the proposed methods for surface reconstruction perform well on sparse noisy range data. In addition, the volume between two surfaces normalized by the surface area (interpreted as average distance between two surfaces) is proposed as an invariant measure for the comparison of reconstruction results.**

***Index Terms*—surface reconstruction, regularization, invariance, preservation of discontinuities, robustness, invariant measure.**

I. Introduction

A. Background

Considerable research has been devoted to the problem of the reconstruction of visible surfaces. Surface reconstruction is necessary to derive a complete representation of a surface from sparse noisy sets of geometric information such as depth and orientation. A reconstructed surface is an intermediate representation to bridge the gap between sensor data and a symbolic description of a surface. An ideal algorithm for reconstruction should have several properties. First, reconstruction must be invariant with respect to viewpoint, that is, to rotations and translations of the surfaces being reconstructed. This is especially important when reconstruction is part of an object recognition system. In this case a change in this intermediate representation may cause a change in any symbolic description that is derived, resulting in failure to identify objects in a scene. Second, it is desirable to find discontinuities in both depth and orientation. A reconstruction algorithm, if detection of discontinuities is not simultaneously carried out in the reconstruction process, should at least sharply preserve regions near discontinuities for a later stage of discontinuity detection. Finally, a reconstruction algorithm should be computationally efficient.

In this paper, we apply regularization techniques using first order convex energy functionals to the problem of surface reconstruction.

Manuscript received June 17, 1993; revised January, 1995.

J.H. Yi is with the Visualization and Intelligent Systems Laboratory, University of California, Riverside, CA 92521.

D.M. Chelberg is with the Geometric Modeling and Perceptual Processing Laboratory, School of Electrical Engineering, Purdue University, West Lafayette, IN 47907; e-mail dmc@ecn.purdue.edu.

IEEECS Log Number P95068.

We propose a novel, computationally efficient form of energy functional for surface reconstruction that achieves approximate invariance, sharp preservation of discontinuities, and robustness with respect to the smoothing parameter λ. That is, reconstruction results do not appreciably degrade as the smoothing parameter λ gets large. This property is significant in that we can freely choose the smoothing parameter λ without struggling to determine the λ that provides the best reconstruction result.

Invariant reconstruction of surfaces in the context of regularization has been investigated by approximating an invariant energy function. Second order models that are capable of invariant reconstruction are investigated in [1], [6]. Blake and Zisserman [1] used a convex approximation to the explicit expression of a second order invariant form and Stevenson and Delp [6] made a convex approximation to the parametric form. However, a convex approximation to the first order invariant form has not been previously reported. This is an important case to consider because first order methods are more computationally efficient than high order methods. In addition, approaches for invariant reconstruction of surfaces do not explicitly consider sharp preservation of discontinuities.

Many researchers have attempted to reconstruct surfaces with sharp preservation of discontinuities. Most efforts toward discontinuity-preserving reconstruction share a common property. Preservation of discontinuities is achieved by properly choosing weighting functions so that the adjacent pixels or the basis functions for spline that are more likely to belong to different regions are less or not weighted in the computation of a reconstructed pixel value. Discontinuities are detected during the reconstruction process by adding to an energy (cost) function a term that depends on the number or extent of the discontinuities [5], [1], [2]. However, this makes the problem nonconvex, and finding the solution is computationally expensive and a global minimum may not be found. Some researchers have detected discontinuities in a preprocessing step for before surface reconstruction [8], [3]. However, none of these methods considers invariance of the reconstruction result at the same time. A detailed description of past work on discontinuity-preserving reconstruction is found in [10].

B. Overview

We employ a first order model instead of a second order model because first order models entail significantly less ($\approx$ an order of magnitude) computational effort than second order models. Surface reconstruction results are compared using an invariant quantitative measure together with visual displays of the reconstruction results. The volume between two surfaces normalized by the surface area is used as an invariant quantitative measure for comparing surface reconstruction results. This measure is invariant with respect to rotations and translations of coordinate system.

The algorithm for surface reconstruction consists of three steps: an initial reconstruction, partial derivative estimates from the initial reconstruction result, and then a second reconstruction which uses the estimated derivatives. The estimated derivatives are inserted as constants into an approximately invariant energy functional (second reconstruction) which makes it convex. The importance of the estimated derivatives is that they improve the performance of the second reconstruction with respect to invariance and preservation of discontinuities. The use of estimated derivatives that are not invariant does not yield truly invariant reconstruction. However, a significant improvement in invariance can be achieved in the second reconstruction even by using this noninvariant information. A similar technique was employed by Blake and Zisserman [1], [2]. In order to estimate the derivatives, we reconstruct the input surface using a simple membrane regularization technique. However, any other appropriate method can be used to produce the derivative estimates. The estimates, $\hat{z}_x$ and $\hat{z}_y$, obtained from the reconstruction results of the simple membrane model are provided for the second invariant and discontinuity-preserving reconstruction of the original noisy range input data (dense or sparse). As long as the derivatives are reasonably accurate, our method is robust and yields good reconstruction results.

The major contribution of this work is a new computationally efficient technique for reconstruction of visible surfaces using a first order energy functional that achieves invariance, preservation of discontinuities, and robustness to the smoothing (or equivalently scale) parameter λ. Our method is based on the explicit representation of surfaces as opposed to parametric representations. We use the explicit form because it typically involves less computation.

II. Viewpoint Invariant Reconstruction

As mentioned in Section I, surface reconstruction that is not invariant with respect to viewpoint may produce different symbolic descriptions, resulting in failure to identify an object in a scene. If the energy functional has a unique global minimum and is invariant to rotations and transformations of the constraints, then the reconstructed surface will also be invariant. Invariance of an energy functional may be achieved by finding an invariant stabilizer and an invariant metric on the constraint space. In this section, we develop invariant energy functions that are employed for the data compatibility measure (Section II.A) and the stabilizing function (Section II.B).

A. Invariant Metric for Data Compatibility Term

Depth constraint data in an explicit form, $z(x, y)$, is used in our work given sparse range data z_{ij}. When a parametric form, $(x(u, v), y(u, v), z(u, v))$, is employed, the same reconstruction process must be carried out for the x, y, and z components, making this approach computationally expensive. Fortunately, for the explicit form, the perpendicular distance[2] $|z - c| \cos \phi$ is invariant under the assumption that the surface, z, and the constraint surface, c, are roughly parallel, where $\cos \phi$ is the surface slant [2]. The squared distance, $(z - c)^2 \cos^2 \phi$, which is also invariant, is used in our work. The data compatibility term $E(z, D)$ is as follows. For surface reconstruction,

$$E(z, D) = \sum_{i,j} \left(z_{i,j} - c_{i,j}\right)^2 \cos^2 \phi = \sum_{i,j} \left(z_{i,j} - c_{i,j}\right)^2 \frac{1}{1 + z_x^2 + z_y^2} \quad (1)$$

where z_x and z_y are the first order derivative at the measurement location (i, j). Estimates, $\hat{z}_x$ and $\hat{z}_y$, of z_x and z_y are inserted as constants in the computation. Equation (1) describes our assumption that noise is greater in regions with high slope. Here the assumption is that, in an image, more steeply inclined surfaces show greater noise than horizontal surfaces. If noise is uniformly distributed in the direction of the normal to a surface, when the surface is imaged from a particular viewpoint, then more steeply inclined regions will have greater uncertainty in their measurements. This agrees with the research result by Ikeuchi and Kanade [4] where they reported a noise model of typical light-stripe range finder. According to their findings, the larger the angle between the surface normal and the illuminator direction of a light stripe, the larger the uncertainty in the sensed z value.

B. Approximately Invariant First Order Stabilizing Function

We present a first order stabilizing function that is both convex and

1. This is the exact distance between the surface, z, and the constraint surface, c. The issue of exact distance in the case of an implicit form of surface is studied in [7].

approximately invariant. We make a convex approximation to the following first order stabilizing function that is nonconvex and invariant.

$$E_p(\mathbf{Z}) = \iint_\Omega \left(\sqrt{1+z_x^2+z_y^2}-1\right)dx\,dy \tag{2}$$

$\Omega \subset \Re^2$ denotes the image domain. A convex approximation to (2) that has been commonly used is as follows:

$$E_p(\mathbf{Z}) = \iint_\Omega \left(z_x^2+z_y^2\right)dx\,dy, \tag{3}$$

which assumes $z_x \approx 0$ and $z_y \approx 0$. This approximation (3) to the invariant stabilizing function (2) is a reasonable choice because it gives a smaller approximation error than higher order expansions as the slope, $z_x^2+z_y^2$, increases. But the approximation error of first order expansion is not ignorable when the slope, $z_x^2+z_y^2$ is large, i.e., surfaces of an image are steep. Our goal is to reduce this approximation error. One obvious choice is to use a higher order expansion of Taylor series at $g=\hat{g}$ where g is $z_x^2+z_y^2$ and $\hat{g}$ is its estimate. If we can come up with a reliable estimate of $\hat{g}$ over an image, then we can reduce the approximation error and achieve an invariant function. However, employing a high order expansion not only produces a nonlinear system but also causes approximation error to be amplified in those higher order terms. The error is especially pronounced in noisy situations. Therefore, our choice of approximation is to use a first order expansion of the Taylor series at $g=\hat{g}$ instead of at $g=0$. The approximation becomes:

$$\sqrt{1+z_x^2+z_y^2}\Big|_{\text{at } z_x^2+z_y^2=\hat{g}} \approx \sqrt{1+\hat{g}} + \frac{1}{2\sqrt{1+\hat{g}}}\left(z_x^2+z_y^2-\hat{g}\right). \tag{4}$$

We use a stabilizing function using this approximation and the data compatibility measure (1) to obtain a novel form of energy function.

III. Discontinuity-Preserving Reconstruction

In the following section, we describe the discretized form of the energy functional and two basic schemes of estimating derivatives (positionally biased and unbiased). The effect of the two different methods of estimating derivatives on the reconstruction results is presented in Section III.B.

A. The Discrete Equations

For simplicity, we use the *forward finite difference* discretized to approximate a continuous surface although it is possible to discretize the surface using a variety of finite elements.

$$\hat{z}_x = \frac{1}{h_x}\left(z_{i,j+1}-z_{i,j}\right) \quad \text{and} \quad \hat{z}_y = \frac{1}{h_y}\left(z_{i+1,j}-z_{i,j}\right). \tag{5}$$

This discretization follows a regular Cartesian sampling pattern typical of images. The image domain $\Omega \subset \Re^2$ is tessellated into rectangular subdomains with sides of h_x and h_y in the x and y directions, respectively. Nodes are located at subdomain corners where they are shared by adjacent subdomains.

Combining the data compatibility measure and the stabilizing function discretized using the finite difference (5), we obtain

$$E^\lambda(\mathbf{Z}) = \sum_{i,j} l_{i,j}\frac{1}{1+\hat{g}_{i,j}}\left(z_{i,j}-c_{i,j}\right)^2 + \lambda^2\sum_{i,j}\frac{1}{\sqrt{1+\hat{g}_{i,j}}}\left\{\frac{1}{h_x^2}\left(z_{i,j+1}-z_{i,j}\right)^2+\frac{1}{h_y^2}\left(z_{i+1,j}-z_{i,j}\right)^2\right\}. \tag{6}$$

where $\hat{g}_{i,j}$ is the estimate of $z_x^2+z_y^2$ at the location of node (i,j) and $l_{i,j}$ is zero where no data is provided at the location of (i,j). Constant terms are ignored. The resulting successive over relaxation (SOR) updating equations for inside pixels are as follows:

If there is data at node (i,j), i.e., $l_{i,j}=1$,

$$z_{i,j}^{n+1} = z_{i,j}^n - \frac{\omega}{a+b\lambda^2}\left[\left(a+b\lambda^2\right)z_{i,j}^n - \frac{1}{1+\hat{g}_{i,j}}c_{i,j} - \lambda^2\left(\frac{z_{i,j-1}^{n+1}}{h_x^2\sqrt{1+\hat{g}_{i,j-1}}}+\frac{z_{i-1,j}^{n+1}}{h_y^2\sqrt{1+\hat{g}_{i-1,j}}}+\frac{z_{i,j+1}^{n}}{h_x^2\sqrt{1+\hat{g}_{i,j}}}+\frac{z_{i+1,j}^{n}}{h_y^2\sqrt{1+\hat{g}_{i,j}}}\right)\right] \tag{7}$$

otherwise, i.e., $l_{i,j}=0$,

$$z_{i,j}^{n+1} = z_{i,j}^n - \frac{\omega}{b}\left[bz_{i,j}^n - \left(\frac{z_{i,j-1}^{n+1}}{h_x^2\sqrt{1+\hat{g}_{i,j-1}}}+\frac{z_{i-1,j}^{n+1}}{h_y^2\sqrt{1+\hat{g}_{i-1,j}}}+\frac{z_{i,j+1}^{n}}{h_x^2\sqrt{1+\hat{g}_{i,j}}}+\frac{z_{i+1,j}^{n}}{h_y^2\sqrt{1+\hat{g}_{i,j}}}\right)\right] \tag{8}$$

where

$$a = \frac{1}{1+\hat{g}_{i,j}}$$

$$b = \frac{1}{h_x^2\sqrt{1+\hat{g}_{i,j-1}}}+\frac{1}{h_y^2\sqrt{1+\hat{g}_{i-1,j}}}+\frac{1}{h_x^2\sqrt{1+\hat{g}_{i,j}}}+\frac{1}{h_y^2\sqrt{1+\hat{g}_{i,j}}}$$

and ω is the overrelaxation parameter of the SOR method. The SOR updating equations when the ordinary membrane (3) is used are found in [2].

Given a novel form of the energy function (6), an interesting problem is how to estimate the gradient, $\hat{g}_{i,j}=\hat{z}_x^2+\hat{z}_y^2$ at the location of node (i,j). Two basic schemes that are commonly used are as follows: One is the forward difference which is a positionally biased estimate of the derivative. It computes $\hat{z}_x$ and $\hat{z}_y$ at the location of (i,j) as

$$\hat{z}_x = \frac{1}{h_x}\left(z_{i,j+1}-z_{i,j}\right) \quad \text{and} \quad \hat{z}_y = \frac{1}{h_y}\left(z_{i+1,j}-z_{i,j}\right). \tag{9}$$

This is the scheme used in the discretization of the energy. Another estimate that is not positionally biased is the central difference obtained as

$$\hat{z}_x = \frac{1}{2h_x}\left(z_{i,j+1}-z_{i,j-1}\right) \quad \text{and} \quad \hat{z}_y = \frac{1}{2h_y}\left(z_{i+1,j}-z_{i-1,j}\right). \tag{10}$$

This problem can be conceived as a *tuning* problem because the reconstruction performance may degrade on the disagreement of the weighting pattern of the updating equation with the method of estimating the derivative. In the next subsection, we will describe the preservation of discontinuities and show the overall reconstruction performance to see how these two different methods of estimating the derivative affect the reconstruction results.

B. Preservation of Discontinuities

It is easy to see that the biased estimate (9) is more appropriate than the unbiased estimate (10) for the purpose of preservation of discontinuities when the updating equations (7) and (8) from the energy (6) are adopted for reconstruction of surfaces. In the case of the unbiased estimate (10), uniform averaging of adjacent nodal values occurs, resulting in blurring across discontinuities.

In fact, the asymmetrical distribution of weighting pattern around the node to be updated in (7) and (8) is not optimal for the unbiased estimates (10) for the purpose of preservation of discontinuities. $z_{i,j+1}^n$ and $z_{i+1,j}^n$ are weighted by the gradient information at (i,j) which is not the gradient information at their own locations. We resolve this

problem by using $\hat{g}_{i,j+1}$ for $\hat{g}_{i,j}$ and $\hat{g}_{i+1,j}$ for $\hat{g}_{i,j}$ assuming a smooth surface. Then the energy becomes

$$E^{\lambda}(\mathbf{Z}) = \sum_{i,j} l_{i,j} \frac{1}{1+\hat{g}_{i,j}} \left(z_{i,j} - c_{i,j}\right)^2 + \lambda^2 \left\{ \cdots + \frac{(z_{i,j+1} - z_{i,j})^2}{h_x^2 \sqrt{1+\hat{g}_{i,j+1}}} + \frac{(z_{i+1,j} - z_{i,j})^2}{h_y^2 \sqrt{1+\hat{g}_{i+1,j}}} + \frac{(z_{i,j} - z_{i,j-1})^2}{h_x^2 \sqrt{1+\hat{g}_{i,j-1}}} + \frac{(z_{i-1,j} - z_{i,j})^2}{h_y^2 \sqrt{1+\hat{g}_{i-1,j}}} + \cdots \right\} \tag{11}$$

The convexity property is not changed because the energy is still expressed as a sum of positive squared terms. The resulting SOR updating equations for the inside pixels are as follows:

If there is data at node (i,j), i.e., $l_{i,j} = 1$.

$$z_{i,j}^{n+1} = z_{i,j}^{n} - \frac{\omega}{a+b\lambda^2} \left[\left(a+b\lambda^2\right) z_{i,j}^{n} - \frac{1}{1+\hat{g}_{i,j}} c_{i,j} - \lambda^2 \left(\frac{z_{i,j-1}^{n+1}}{h_x^2 \sqrt{1+\hat{g}_{i,j-1}}} + \frac{z_{i-1,j}^{n+1}}{h_y^2 \sqrt{1+\hat{g}_{i-1,j}}} + \frac{z_{i,j+1}^{n}}{h_x^2 \sqrt{1+\hat{g}_{i,j+1}}} + \frac{z_{i+1,j}^{n}}{h_y^2 \sqrt{1+\hat{g}_{i+1,j}}} \right) \right] \tag{12}$$

otherwise, i.e., $l_{i,j} = 0$,

$$z_{i,j}^{n+1} = z_{i,j}^{n} - \frac{\omega}{b} \left[b z_{i,j}^{n} - \left(\frac{z_{i,j-1}^{n+1}}{h_x^2 \sqrt{1+\hat{g}_{i,j-1}}} + \frac{z_{i-1,j}^{n+1}}{h_y^2 \sqrt{1+\hat{g}_{i-1,j}}} + \frac{z_{i,j+1}^{n}}{h_x^2 \sqrt{1+\hat{g}_{i,j+1}}} + \frac{z_{i+1,j}^{n}}{h_y^2 \sqrt{1+\hat{g}_{i+1,j}}} \right) \right] \tag{13}$$

where

$$a = \frac{1}{1+\hat{g}_{i,j}}$$

$$b = \frac{1}{h_x^2 \sqrt{1+\hat{g}_{i,j-1}}} + \frac{1}{h_y^2 \sqrt{1+\hat{g}_{i-1,j}}} + \frac{1}{h_x^2 \sqrt{1+\hat{g}_{i,j+1}}} + \frac{1}{h_y^2 \sqrt{1+\hat{g}_{i+1,j}}}.$$

We compare the following three reconstructions:

- FIT: ordinary reconstruction using the ordinary membrane model (3).
- IDFIT-BIASED: invariant and discontinuity-preserving reconstruction using the updating equations (7) and (8) with the biased estimates (9).
- IDFIT-UNBIASED: invariant and discontinuity-preserving reconstruction using the updating equations (12) and (13) with the unbiased estimates (10).

We have computed the weighting patterns of the edge pixels for the cases of IDFIT-BIASED and IDFIT-UNBIASED for various patterns of discontinuities. The comparison of the weighting patterns for the edge pixels alone may lead to a careless conclusion that IDFIT-BIASED is better at preservation of discontinuities than IDFIT-UNBIASED. However, the weighting patterns of the pixels next to the edge pixels play a more important role than those of the edge pixels in the overall reconstruction performance as well as in the reconstruction of pixel values at the edge locations. In short, IDFIT-UNBIASED produces less reconstruction error than IDFIT-BIASED because edge nodes of IDFIT-UNBIASED can maintain sharper contrast than those of IDFIT-BIASED. Nodes next to edge nodes are less blurred in the previous iteration in the case of IDFIT-UNBIASED than IDFIT-BIASED. This local phenomenon propagates throughout the entire image and this is the reason for the better reconstruction of IDFIT-UNBIASED than that of IDFIT-BIASED. The same behavior is observed for all directions of discontinuity as seen in the results of Fig. 1. This performance result has been verified with the test images used in the experiments presented in the results section. A detailed discussion of the weighting patterns of the three reconstruction methods is given in [10].

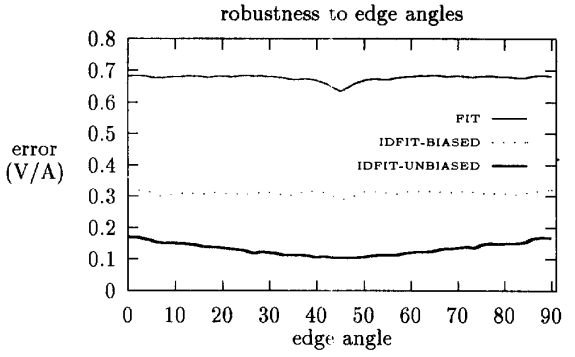

Fig. 1. The performance of FIT, IDFIT-BIASED, and IDFIT-UNBIASED for various directions of a step discontinuity.

IV. Experimental Results

A. Test Data

Two synthetic (size 128 × 128) and two actual (size 240 × 240) range images shown in Fig. 2 are used for the experiments. Sparse images are generated by randomly deleting pixels of a dense noisy image. The curved-inclined image has three flat, two inclined (slope 1 and $\frac{1}{2}$) and two curved surfaces (curvature $\frac{1}{20}$ and $\frac{1}{30}$) and is used to show the performance of the three reconstruction methods as the amount of noise varies. Noise is added in the direction of the surface normal vector. To test for invariance, we use DATA1 and DATA2. DATA1 and DATA2 have two inclined planes of which the slopes are tan 15° and tan 75°. DATA2 is obtained by rotating DATA1 by 60 degrees about the y-axis. $N(0, 1)$ is added to DATA1 and DATA2 in the direction of the surface normal vector. In order to show the invariance property, dense and sparse DATA1 and DATA2 that are noisy are reconstructed and the reconstructed result for DATA2 is rotated back into correspondence with DATA1. The difference between the two reconstructed surfaces is examined by computing the volume between them divided by the average surface area of the two reconstructions.

B. Invariant Performance Measure

The metrics induced by the L^1, L^2, or L^∞ norms have been popularly used in order to give a quantitative measure for comparison of reconstruction results. The use of these metrics has often naturally resulted because some reconstruction methods employ minimization techniques of L^1, L^2, or L^∞ error between the true or target data set and the measurement data set (constraints) to compute the reconstruction results. These metrics, however, are not invariant with respect to a coordinate system when applied to surfaces in explicit form, resulting in different measures for different coordinate systems. It is clear that if the L^2 metric is used as a difference measure, the difference value is emphasized more in regions where the slope is high than in flat regions.

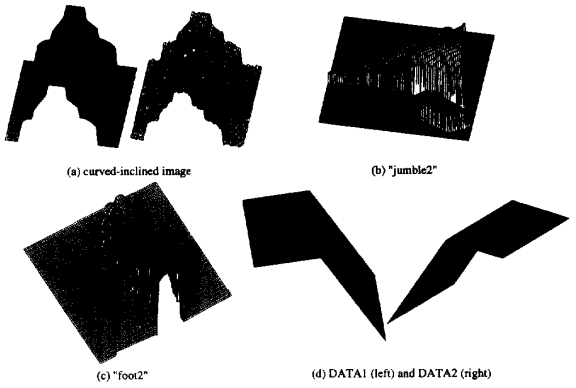

Fig. 2. Three-dimensional displays of images used in the experiments.

We use V/A as an invariant performance measure for the comparison of reconstruction results, where V represents the volume between two surfaces and A the surface area. We have developed a simple and efficient method to compute the volume between two surfaces and the surface area. See [9] for details. It is important to point out that other measures such as $V^{\frac{1}{3}} / A^{\frac{1}{2}}$ could be used to give a dimensionless measure. These measures, however, do not have an intuitive relation to geometry as does V / A (average distance between surfaces).

C. Reconstruction Results

Fig. 3 shows the reconstruction results of the actual range image, "foot2." The figure clearly shows that IDFIT-UNBIASED performs better than IDFIT-BIASED in preservation of discontinuities. Notice the difference in V/A values. Results showing the robustness of the method with respect to various λ (for the ranges of λ (0.0 ~ 5.0)) are reported in Fig. 4 using "jumble2" for both dense and sparse cases. The robustness property of IDFIT-UNBIASED is clearly demonstrated. IDFIT-BIASED results in more and more blurring as λ gets large in contrast to the performance of IDFIT-UNBIASED whose performance does not appreciably degrade. Fig. 5 illustrates the results of invariance tests by comparing one slice of the reconstruction results. The invariance performance of IDFIT-UNBIASED and IDFIT-BIASED is not much different from each other. On the other hand, FIT performs worse than IDFIT-UNBIASED and IDFIT-BIASED with respect to invariance. When the data is dense, the reconstructed surface follows the data closely for all three reconstructions as shown in Fig. 5(a). However, the difference in the invariance property between FIT and IDFIT-UNBIASED and IDFIT-BIASED is still visible. As the sparseness of input image increases (i.e., when there are fewer data points), the invariance performance of FIT gets much worse than that of IDFIT-UNBIASED and IDFIT-BIASED. See Fig. 5(b) where 90% of the pixels are missing. Invariance of IDFIT-UNBIASED (V/A = 0.2971) and IDFIT-BIASED (V/A = 0.3340) is much better than FIT (V/A = 0.7070). For Fig. 2(a), under conditions of 80% sparseness IDFIT-UNBIASED (V/A = 0.3265) (V/A = 0.6745) which is better than FIT.

V. Conclusion

In contrast to previous work, the first order energy functional with positionally unbiased derivative estimates presented here for surface reconstruction is the first first-order computationally efficient method to achieve both preservation of discontinuities and approximate invariance. It also has the important property of robustness to the smoothing parameter λ. These properties along with computational efficiency make the proposed method for surface reconstruction more attractive than other existing methods. It works especially well on sparse noisy range data. Other methods may perform better either in invariance or in preservation of discontinuities, however, they are not as efficient as our first order method because they employ second order models or detect discontinuities during the reconstruction process. In addition, they do not achieve both invariance and preservation of discontinuities.

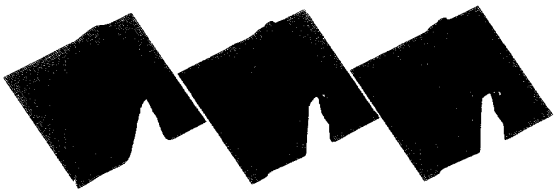

Fig. 3. Reconstruction results of "foot2" when $\lambda = 5.0$.

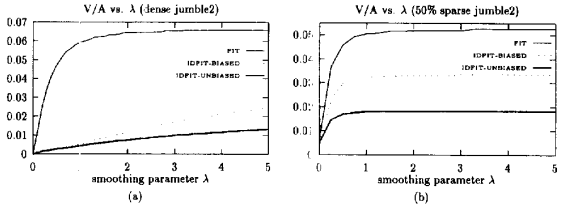

Fig. 4. Robustness with respect to the smoothing parameter λ.

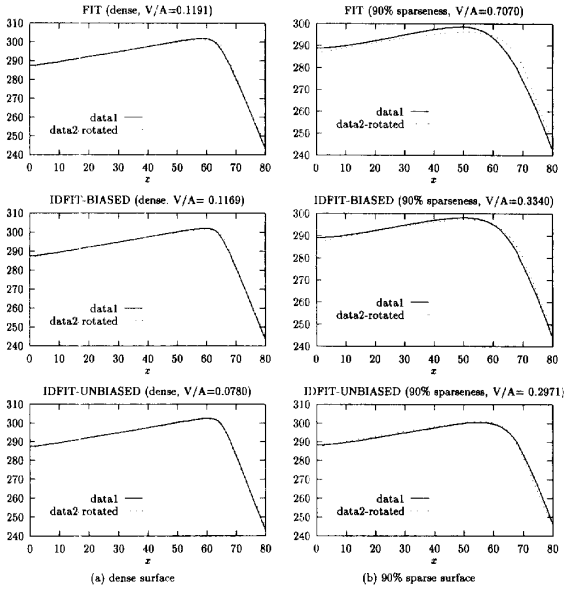

Fig. 5. Invariance performance of FIT, IDFIT-BIASED, and IDFIT-UNBIASED, $\lambda = 3.0$. In order to show the invariance performance of three methods, dense and sparse DATA1 and DATA2 that are noisy are reconstructed and the reconstructed result for DATA2 is rotated back into correspondence with DATA1. Comparison of a section of the reconstruction results is displayed. The vertical axis represents z value.

ACKNOWLEDGMENTS

The authors gratefully acknowledge Michigan State University's Pattern Recognition and Image Processing Laboratory for the range images "jumble2" and "foot2" used in this work.

This work was supported by a Digital Equipment Corporation Faculty Incentives for Excellence Grant, and by NSF Grant number IRI-9011421.

REFERENCES

[1] A. Blake and A. Zisserman, "Invariant surface reconstruction using weak continuity constraints," *Proc. IEEE Int'l Conf. Computer Vision Pattern Recognition*, Miami, Florida, pp. 22–26, June 1986.

[2] A. Blake and A. Zisserman, *Visual Reconstructions*. Cambridge, Mass.: MIT Press, pp. 93, 110, 1987.

[3] D.M. Chelberg and J. Yi, "Range image segmentation using regularization," *Proc. SPIE Int'l Conf. Intelligent Robot Advanced Systems*, Boston, Mass., pp. 336–347, Nov. 1991.

[4] K. Ikeuchi and T. Kanade, "Modeling sensors and applying sensor model to automatic generation of object recognition program," *Proc. DARPA Image Understanding Workshop*, pp. 697–710, 1987.

[5] D. Mumford and J. Shah, "Boundary detection by minimizing functionals," *Proc. IEEE Int'l Conf. Computer Vision Pattern Recognition*, San Francisco, Calif., 1985.

[6] R.L. Stevenson and E.J. Delp, "Viewpoint invariant recovery of visual surfaces from sparse data," *IEEE Trans. Pattern Analysis Machine Intellience*, vol. 14, pp. 897–909, Sept. 1992.

[7] G. Taubin, "An improved algorithm for algebraic curve and surface fitting," *Proc. Fourth Int'l Conf. Computer Vision*, Berlin, Germany, pp. 658–665, May 1993.

[8] D. Terzopoulos, "The computation of visible-surface representations," *IEEE Trans. Pattern Analysis Machine Intelligence*, vol. 10, pp. 417–438, July 1988.

[9] J. Yi and D.M. Chelberg, "Computation of volume and surface area over grid sampled surfaces," Technical Report TR-93-31, School of Electrical Engineering, Purdue University, West Lafayette, Indiana, 1993.

[10] J. Yi and D.M. Chelberg, "Invariant reconstruction of curves and surfaces using a first order regularization," Technical Report TR-93-30, School of Electrical Engineering, Purdue University, West Lafayette, Indiana, 1993.

Subpixel Edge Location in Binary Images Using Dithering

Xiangdong Liu and Roger W. Ehrich

***Abstract*—This paper concerns the problem of obtaining subpixel estimates of the locations of straight edges in binary digital images using dithering. By adding uniformly distributed independent random noise it is shown that estimation bias may be removed and that the estimation variance is inversely proportional to the length of the line segment. The sensitivity to incorrect dither amplitude is calculated, and implementation is discussed.**

***Index Terms*—Dither, edge, inspection, subpixel.**

I. INTRODUCTION

Subpixel edge location measurement is extremely important for machine inspection and mensuration applications. It permits highly accurate measurements to be made with inexpensive, low resolution vision sensors. In many cases physical constraints do not permit the use of higher resolution sensors, and one must strive to achieve the best possible accuracies with limited sensor capabilities. A large number of papers have appeared in the last decade concerning a broad range of subpixel edge location techniques for diverse applications. Generally these have been obtained with widely varying assumptions, and it is not always easy to understand what they are. For the gray-level techniques [1], [2], [3], [4], [5], [6], [7], the performance is not usually known analytically. Binary techniques suffer from fundamental limitations related to edge orientation. Commonly shared among the various approaches is the idea that the longer the edge being measured, the better the estimates of edge position become. Central limit theorem-like arguments suggest that as n independent edge measurements are made, the variance of position estimators is reduced by the factor $1/n$, with the possible exceptions of rational slopes, most notably vertical, horizontal, or 45° diagonal lines where the measurements are completely correlated.

This paper is motivated by applications in which objects are to be digitized in binary and measured with high accuracy. Binary digitization is desirable for reducing storage requirements and for speeding up computations in applications involving extremely large images. We first show that by adding random position noise to the line or by introducing dither to the sensor, the $1/n$ reduction in variance is preserved, regardless of line orientation. This can be implemented in various ways by actually making ideally straight scene edges fuzzy in the images themselves or equivalently by randomizing the sensor binarization threshold in just the right way. We calculate the worst-case performance and investigate the sensitivity of the estimate to slight deviations from the optimal dither noise statistics.

II. REVIEW OF PREVIOUS WORK

Since binary approaches are most relevant here, we confine our discussions to several of the most notable results.

Dorst and Smeulders [8] were interested specifically in the geometrical properties of binarized lines of finite length. For example, they characterized the set of continuous finite length line segments which, after digitization, give rise to the same digital line segment with a particular chain code. Later, Dorst and Duin [9] also pointed out that the maximum vertical distance between any two parallel line segments in

Manuscript received Aug. 16, 1993; revised Mar. 8, 1995.

X. Liu and R.W. Ehrich are with the Department of Computer Science, Virginia Polytechnic Institute and State University, Blacksburg, VA 24060.

IEEECS Log Number P95071.